JACS
JOURNAL OF THE AMERICAN CHEMICAL SOCIETY
Communication
pubs.acs.org/JACS

Nickel(II) Dithiocarbamate Complexes Containing Sulforhodamine B as Fluorescent Probes for Selective Detection of Nitrogen Dioxide

Yan Yan,[†] Saarangan Krishnakumar,[†] Huan Yu,[‡] Srinivas Ramishetti,[§] Lih-Wen Deng,[∥] Suhua Wang,*[,‡] Leaf Huang,[§] and Dejian Huang*[,†]

[†]Department of Chemistry, National University of Singapore, 3 Science Drive 3, Singapore 117543, Singapore

[‡]Institute of Intelligent Machines, Chinese Academy of Sciences, Hefei, Anhui 230031, China

[∥]Department of Biochemistry, Yong Loo Lin School of Medicine, National University of Singapore, National University Health System, 8 Medical Drive, Singapore 117597, Singapore

[§]Division of Molecular Pharmaceutics, Eshelman School of Pharmacy, University of North Carolina at Chapel Hill, Chapel Hill, North Carolina 27599, United States

Supporting Information

ABSTRACT: We synthesized complexes of Ni(II) with dithiocarbamate ligands derived from the ortho and para isomers of sulforhodamine B fluorophores and demonstrated they are highly selective in reactions with nitrogen dioxide (NO_2). Compared with the para isomer, the ortho isomer showed a much greater fluorescence increase upon reaction with NO_2, which led to oxidation and decomplexation of the dithiocarbamate ligand from Ni(II). We applied this probe for visual detection of 1 ppm NO_2 in the gas phase and fluorescence imaging of NO_2 in macrophage cells treated with a nitrogen dioxide donor.

As a dominant component in the NO_x (x = 1, 2) family, nitrogen dioxide (NO_2) is a major air pollutant generated from high-temperature oxidation of N_2 in combustion.[1] Biologically, NO_2 has been implicated as the root cause of toxic effects of reactive nitrogen species derived from oxidation of nitric oxide (NO) by oxygen in cells[2] and from one-electron reduction of nitrite by metalloenzymes.[3] As an air-stable and strong lipophilic oxidant, NO_2 can trigger lipid auto-oxidation[4] and oxidative nitration of aromatic amino acids, particularly tyrosine.[5] However, there is a lack of selective fluorescent probes for convenient detection of NO_2. Most of the reported fluorescent probes are for NO detection. While probes based on transition-metal complexes contain a NO-reactive metal as a fluorescence quencher,[6−10] organic-dye-based probes detect NO indirectly through oxidation of aromatic amines by N_2O_3,[11,12] which is produced via oxidation of NO by O_2.[13,14] We herein report the first fluorescent probe for selective detection of NO_2, which contains Ni(II) as a fluorescence quencher and NO_2 reaction center.

The reaction of sulforhodamine with oxalyl chloride yielded a mixture of two isomeric compounds having the $-SO_2Cl$ group at the para or ortho position of the phenyl ring.[15] The mixture was treated directly with piperazine, and the two isomers produced were separated readily by column chromatography to give the para isomer, **1**, and the ortho isomer, **2** (Scheme 1). Because of their similarity, it was difficult to distinguish their structures unambiguously on the basis of NMR and mass spectra alone. Hence, the structures were determined by single-crystal X-ray diffraction [Figure S1 in the Supporting Information (SI)], and accordingly, the ^{1}H NMR spectral data were assigned with certainty. In the presence of sodium hydroxide, the two isomers reacted readily with carbon disulfide to produce the sodium dithiocarbamate salts **3** and **4**, respectively. Dithiocarbamate is a bidentate ligand that promptly forms complexes with many transition metals, leading to quenching of the ligand fluorescence. It has been reported that Ni(II) bis(dithiocarbamate) complexes, $Ni(RNCS_2)_2$, react immediately with NO_2 to yield the oxidatively dimerized ligand, $(RNCS_2)_2$,[16] which can be fluorescent if R is a fluorophore. Hence, to prepare Ni(II)-based turn-on fluorescent probes for NO_2, we mixed nickel(II) nitrate with 2 equiv of **3** and **4**, which afforded **5** and **6**, respectively (Scheme 1). The structures of **5** and **6** were characterized by ^{1}H NMR spectroscopy, and the

Scheme 1

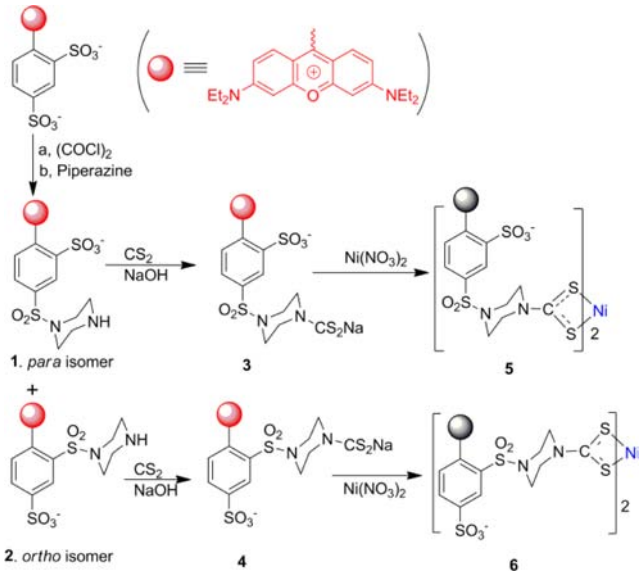

Received: February 12, 2013
Published: March 26, 2013

   dx.doi.org/10.1021/ja401555y | J. Am. Chem. Soc. 2013, 135, 5312−5315

results were in agreement with a diamagnetic nickel complex having a square-planar configuration. Additionally, their MALDI-TOF mass spectra showed isotope distribution patterns matching the expected molecular formula (Figure S2).

To illustrate the effect of the two isomers on fluorescence quenching, the fluorescence quantum yield (QY) of each compound shown in Scheme 1 was measured (Table S1 in the SI). The presence of the piperazine group at the ortho position in **2** (QY = 0.21) reduced the QY relative to the parent compound sulforhodamine B (QY = 0.34) more significantly than having this group at the para position in **1** (QY = 0.28). The addition of dithiocarbamate groups further reduced the quantum yield a little bit. The ortho isomer of the Ni(II) complex, **6**, had the lowest QY, which was 70 times lower than that of ligand **4** alone, while the QY of para isomer **5** was only 5 times than that of the corresponding ligand **3**. Energy transfer is not likely, as there is only a small overlap of the fluorophore emission and quencher absorption bands (Figure S3).

The mechanism behind the fluorescence quenching probably involves photoinduced electron transfer (PET) from the electron donor, Ni(II), to the sulforhodamine B excited state. The energies of the highest-occupied molecular orbital (HOMO) and lowest-unoccupied MO (LUMO) of Ni-$(Me_2NCS_2)_2$ were calculated to be −4.09 and −1.03 eV, respectively, and dithiocarbamate ligands are known to stabilize Ni(III).[17] The HOMO and LUMO energies of rhodamine B are −8.058 and −5.266 eV, respectively,[18] and therefore, PET from Ni to the rhodamine B chromophore is energetically favored. Because PET is highly sensitive to the distance between the fluorophore and the quencher, the shorter distance from Ni to the center of the fluorophore in **6** is likely to result in a much higher quenching efficiency than for **5**. From the crystal structures of **1** and **2**, the distances from the NH nitrogen in the piperazine group to the center of the fluorophore were calculated to be 9.4 and 7.4 Å, respectively. Although we failed to obtain single-crystal structures of the Ni complexes, it is reasonable to assume that the distance from the Ni to the rhodamine B chromophore would be shorter in **6** than in **5**. It should be borne in mind that in solution, molecular motions will have a significant effect on the distances.

We evaluated the selectivity of the ortho isomer **6** toward common reactive oxygen species (ROS) in methanol (Figure S5). Only NO_2 could increase the fluorescence intensity more than 12-fold, whereas other biological relevant ROS could not do so. Neither nitrite nor nitrate could switch on the fluorescence. Moreover, addition of the NO donor diethylamine NONOate (DEANO) rapidly turned on the fluorescence 12-fold within minutes, and there was an excellent dose−response relationship between the fluorescence intensity and the DEANO concentration (Figure S7). In comparison, when the para isomer **5** was used, the magnitude of the fluorescence increase was only 1.9-fold (Figure S6). Although there is a sulfonate group on the fluorophore of probe **6**, its water solubility is extremely poor. In aqueous media (water and buffer), there was no fluorescence intensity gain after addition of NO_2. It turned out that the reaction products precipitated out even at the micromolar concentration level used in the experiment. Addition of a surfactant (Tween 20) to the reaction mixture before addition of NO_2 led to fluorescence turn-on. Therefore, to introduce the probe under physiological conditions, we applied 1,2-dioleoyl-3-trimethylammoniumpropane chloride salt (DOTAP) liposomes as a delivery vehicle for our probe. It was found that probe **6** delivered using DOTAP demonstrated excellent selectivity for NO_2 (Figure 1) and a good dose−response relationship to DEANO (Figure 2) in buffered aqueous media to simulate physiological conditions.

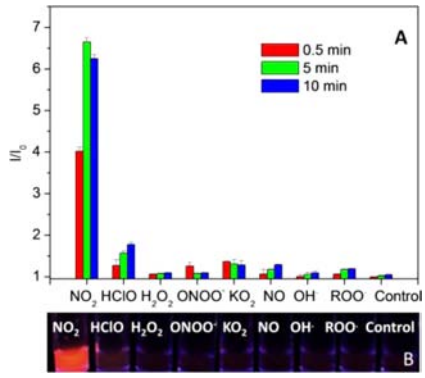

Figure 1. Ortho isomer **6** is selective toward common ROS under physiological conditions. (A) Fluorescence responses obtained upon addition of various ROS (1 μM) to **6** (0.2 μM) delivered using 20 equiv of DOTAP in 10 mM PBS (pH 7.4) at 37 °C (λ_{ex} = 540 nm, λ_{em} = 590 nm). (B) Digital photos showing that NO_2 turns on the fluorescence but other ROS do not under illumination by a 365 nm UV lamp 5 min after addition of ROS (5 μM) to **6** (1 μM) delivered using 20 equiv of DOTAP in 10 mM PBS (pH 7.4).

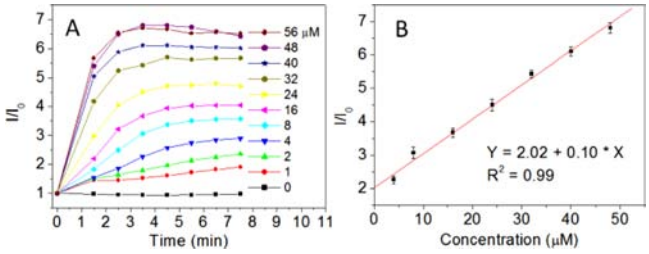

Figure 2. Responses of ortho isomer **6** to DEANO at different concentrations under physiological conditions. (A) Increments of fluorescence intensity of **6** (0.2 μM) delivered using 20 equiv of DOTAP against time after the addition of DEANO at different concentrations in 10 mM PBS (pH 7.4) at 37 °C (λ_{ex} = 540 nm, λ_{em} = 590 nm). (B) Dose−response curve for the fluorescence intensity of **6** (0.2 μM) delivered using 20 equiv of DOTAP obtained 3.5 min after the addition of DEANO in 10 mM PBS (pH 7.4) at 37 °C (λ_{ex} = 540 nm, λ_{em} = 590 nm).

As a further test of whether the probe is sensitive to NO or NO_2, we carried out the reaction in the absence of oxygen by degassing the probe solutions and DEANO solutions before mixing them under nitrogen, and we failed to observe any fluorescence turn-on event. This observation showed that the fluorescence turn-on by DEANO required oxygen, suggesting that it is NO_2 that reacts with the probe as NO generated from DEANO is rapidly oxidized to NO_2 by oxygen present in the solution.[19] This was confirmed by a separate test in which the responses of the probe to NO_2 formed by mixing NO and air and to commercial NO_2 gas were examined. Indeed, the fluorescence was turned on. To verify that the products of the reactions of **6** with DEANO in the presence of air and with NO_2 gas are identical, the reaction products were analyzed using HPLC and LC−MS. The results suggested that the same major products with fluorescence were generated by the reactions of the probe with DEANO in the presence of air and with NO_2 gas in methanol. These results clearly show that NO_2

dx.doi.org/10.1021/ja401555y | J. Am. Chem. Soc. 2013, 135, 5312−5315

can turn on the fluorescence of the probe. Moreover, the para isomer **5** also reacted with NO_2 in the same way as the ortho isomer **6**, as characterized by HPLC chromatograms (Figure 3).

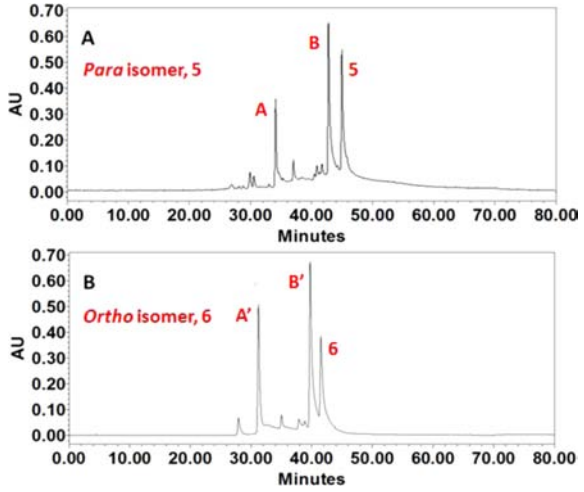

Figure 3. HPLC chromatograms of the products of the reactions of **5** and **6** with NO_2, recorded at 560 nm.

The structures of the reaction products were then deduced on the basis of LC–MS^n spectra, as shown in Scheme 2.

Scheme 2

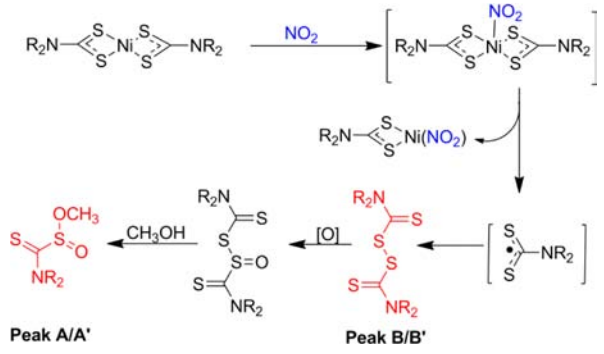

Apparently, NO_2 oxidizes the dithiocarbamate ligand and generates Ni(II)-free compounds that strongly fluoresce. We propose that the reaction is initiated by oxidative formation of an adduct of NO_2 with **5**/**6**, $Ni^{III}(R_2NCS_2)_2(NO_2)$. A subsequent intramolecular electron transfer reaction forms $Ni^{II}(R_2NCS_2)(NO_2)$ and a $R_2NCS_2\cdot$ radical, and these radicals couple to give ligand dimers, which correspond to peak **B**/**B′** (Scheme 2). The compound corresponding to peak **A**/**A′** is generated by a secondary oxidation reaction of $(R_2NCS_2)_2$ followed by methanolysis. Consistent with the two proposed compounds, electrospray ionization mass spectrometry (ESI-MS) analysis of the compound corresponding to peak **A**/**A′** gave an $[M + H]^+$ peak at m/z 749.2 and an $[M + Na]^+$ peak at m/z 771.2, while ESI-MS analysis of the compound corresponding to peak **B**/**B′** demonstrated two dications, $[M + 2H]^{2+}$ at m/z 702.2 and $[M + 2Na]^{2+}$ at m/z 724.2. Our assignments are supported by ESI-MS^2 fragmentation patterns of **A′** and **B′**. The MS^2 spectrum of peak **A′** showed three fragments at m/z 717.1, 669.2, and 637.0 due to $[M + H - CH_3OH]^+$, $[M + H - SO_3]^+$, and $[M + H - CH_3OH - SO_3]^+$, respectively. The MS^2 spectrum of **B′** gave a peak at m/z 627.2 formed from the molecular cation through homolytic cleavage of the S–S bond and subsequent loss of CS_2 (Figure S4).

In addition, the formula of the species corresponding to peaks **A′** and **B′** were confirmed by high-resolution MS (Table S2). Our results are in agreement with literature work, which showed that bis(diethyldithiocarbamato)nickel(II) $[Ni(dtc)_2]$ reacts with NO_2 (but not with NO) to give corresponding paramagnetic complex $Ni^{III}(dtc)_3$ as an intermediate, which decomposes to give the oxidized dithiocarbamate ligand [i.e., thiuram disulfide, $(R_2NCS_2)_2$].[16]

In view of the high toxicity of NO_2 in the atmosphere, the U.K. Health and Safety Executive (HSE) has approved occupational exposure standards of 1 ppm (8 h time-weighted average) and 5 ppm (short-term exposure limit) for NO_2.[20] Convenient detection of gaseous NO_2 would be ideal for monitoring air pollution due to NO_x (x = 1 or 2, with NO_2 being dominant species). For this purpose, probe **6** was successfully applied in visual detection of gaseous NO_2 with a detection limit reaching 1.0 ppm by using NO_2 indicator strips prepared by dropping a 1:1 methanol/chloroform solution of **6** (800 nM) on filter paper to give round stains ca. 5 mm in diameter after solvent evaporation. The NO_2 indicator strips were exposed to different concentrations of NO_2 gas for 10 min. Under regular laboratory light, no apparent spot could be detected on any of the indicator strips (Figure 4 right). When

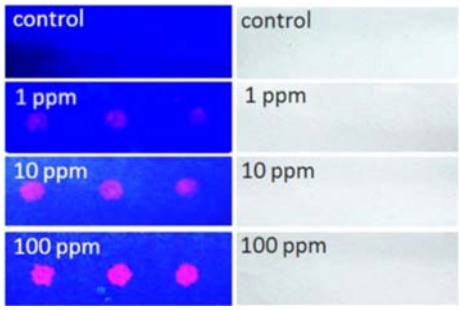

Figure 4. Visual detection of NO_2 gas. NO_2 concentrations of 0, 1, 10, and 100 ppm were tested. The images on the left were obtained under illumination by a 352 nm UV lamp in the dark. For comparison, no color can be seen in the images on the right, which were obtained under laboratory lighting without UV light excitation.

the strips were exposed to a UV lamp (352 nm), red fluorescence spots could be observed visually for strips exposed to NO_2 gas at concentrations as low as 1.0 ppm, and the fluorescence intensity increased in a dose-dependent manner at 10 and 100 ppm NO_2 (Figure 4 left). These results demonstrated that NO_2 indicator strips immobilized with probe **6** can serve as a simple, direct, and economical tool for rapid detection of gaseous NO_2 at low concentrations.

To introduce the probe into a biological system, a liposomal carrier was applied. Cationic liposomes have been studied extensively in gene therapy applications, and cationic lipids are effective in vaccine formulations to treat cancers.[21,22] Therefore, we applied DOTAP liposomes as a delivery vehicle for our probe. Although it is known that DOTAP liposomes at high concentration are toxic to cells, our observations showed that RAW 264.7 cells can withstand up to 100 μM DOTAP (Figure S8). To illustrate that fluorescence from probe **6** uptaken by cells can be turned on by addition of NO_2, RAW 264.7 cells treated with DOTAP liposomes containing **6** (5 μM) were further treated with DEANO as a NO_2 donor.[19] The

dx.doi.org/10.1021/ja401555y | J. Am. Chem. Soc. 2013, 135, 5312–5315

fluorescence images of the cells (Figure 5B,D) clearly illustrate that the fluorescence intensity could be efficiently enhanced by

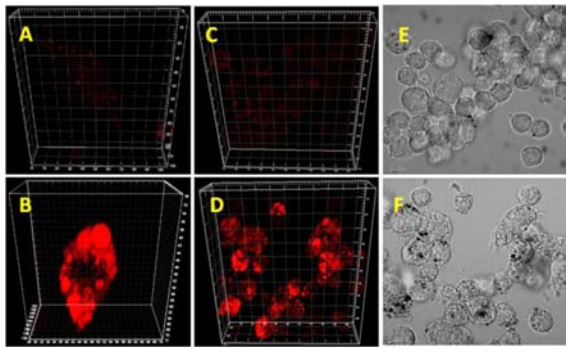

Figure 5. NO_2 turns on the fluorescence of RAW 264.7 cells stained with **6**. (A, B) 3D images of single cells (A) without and (B) with DEANO treatment (1 mM). (C, D) 3D images of groups of cells (C) without and (D) with DEANO treatment (1 mM). (E, F) Bright-field cell images corresponding to (C) and (D).

adding DEANO (for an intensity plot, see Figure S9). Moreover, the *Z*-stack gallery image (Figure S10) clearly shows that probe **6** dispersed in DOTAP was efficiently taken up by RAW 264.7 cells. The 3D images in Figure 5A–D demonstrate the depth distribution of **6** inside cells with and without DEANO treatment.

In conclusion, we have demonstrated that Ni(II) complexes of dithiocarbamate ligands containing sulforhodamine B fluorophores are highly selective probe for detection of NO_2. To the best of our knowledge, this is the first example of live-cell fluorescence imaging of NO_2 activity and visual detection of gaseous NO_2 at low concentrations. Many third-row transition metals are good fluorescence quenchers because their complexes with fluorescent ligands are paramagnetic as a result of the unpaired metal d electrons. In contrast, the Ni(II) coordination spheres in complexes **5** and **6** adopt a square-planar geometry and are diamagnetic. Further research to understand the quenching mechanisms of Ni(II) and develop even more sensitive probes by rational combination of fluorophores and nickel complexes is warranted.

■ ASSOCIATED CONTENT

Ⓢ Supporting Information

Synthetic procedures and spectroscopic data for **1**–**6**, crystal structures of **1** and **2**, and experimental procedures for cell imaging and selectivity of the probe toward different ROS. This material is available free of charge via the Internet at http://pubs.acs.org.

■ AUTHOR INFORMATION

Corresponding Author

shwang@iim.ac.cn; chmhdj@nus.edu.sg

Notes

The authors declare no competing financial interest.

■ ACKNOWLEDGMENTS

D.H. and L.W.D. thank the Agency of Science, Technology and Research (A*Star) of Singapore for financial support (Grant 112 177 0036). D.H. and S.W. thank the National Natural Science Foundation of China for Grant 21228702. L.H. thanks the National Institutes of Health for Grant CA129421.

■ REFERENCES

(1) Bascom, R.; Bromberg, P. A.; Costa, D. A.; Devlin, R.; Dockery, D. W.; Frampton, M. W.; Lambert, W.; Samet, J. M.; Speizer, F. E.; Utell, M. *Am. J. Respir. Crit. Care Med.* **1996**, *153*, 3–50.
(2) Lewis, R. S.; Tamir, S.; Tannenbaum, S. R.; Deen, W. M. *J. Biol. Chem.* **1995**, *270*, 29350–29355.
(3) Bian, K.; Gao, Z.; Weisbrodt, N.; Murad, F. *Proc. Natl. Acad. Sci. U.S.A.* **2003**, *100*, 5712–5717.
(4) Byun, J.; Mueller, D. M.; Fabjan, J. S.; Heinecke, J. W. *FEBS Lett.* **1999**, *455*, 243–246.
(5) Kirsch, M.; Korth, H.-G.; Sustmann, R.; de Groot, H. *Biol. Chem.* **2002**, *383*, 389–399.
(6) Mondal, B.; Kumar, P.; Ghosh, P.; Kalita, A. *Chem. Commun.* **2011**, *47*, 2964–2966.
(7) Hu, X.; Wang, J.; Zhu, X.; Dong, D.; Zhang, X.; Wu, S.; Duan, C. *Chem. Commun.* **2011**, *47*, 11507–11509.
(8) Rosenthal, J.; Lippard, S. J. *J. Am. Chem. Soc.* **2010**, *132*, 5536–5537.
(9) Lim, M. H.; Lippard, S. J. *Acc. Chem. Res.* **2007**, *40*, 41–51.
(10) Wang, S. H.; Han, M. Y.; Huang, D. J. *J. Am. Chem. Soc.* **2009**, *131*, 11692–11694.
(11) Terai, T.; Urano, Y.; Izumi, S.; Kojima, H.; Nagano, T. *Chem. Commun.* **2012**, *48*, 2840–2842.
(12) Kojima, H.; Nakatsubo, N.; Kikuchi, K.; Kawahara, S.; Kirino, Y.; Nagoshi, H.; Hirata, Y.; Nagano, T. *Anal. Chem.* **1998**, *70*, 2446.
(13) Chen, Y.; Guo, W.; Ye, Z.; Wang, G.; Yuan, J. *Chem. Commun.* **2011**, *47*, 6266–6268.
(14) Yang, Y.; Seidlits, S. K.; Adams, M. M.; Lynch, V. M.; Schmidt, C. E.; Anslyn, E. V.; Shear, J. B. *J. Am. Chem. Soc.* **2010**, *132*, 13114–13116.
(15) Hua, Y.; Sundar, V.; Christopher, O. O.; Jay, S.; Rich, G. C. *Synthesis* **2008**, 957–961.
(16) Yordanov, N. D.; Iliev, V.; Shopov, D. *Inorg. Chim. Acta* **1982**, *60*, 17–20.
(17) Bitterwolf, T. E. *Inorg. Chim. Acta* **2008**, *361*, 1319–1326.
(18) Gondal, M. A.; Chang, X.; Al-Saadi, A. A.; Yamani, Z. H.; Zhang, J.; Ji, G. *J. Environ. Sci. Health, Part A* **2012**, *47*, 1192–1200.
(19) Goldstein, S.; Czapsk, G. *J. Am. Chem. Soc.* **1995**, *117*, 12078–12084.
(20) http://www.hse.gov.uk/coshh/basics/exposurelimits.htm.
(21) Srinivas, R.; Samanta, S.; Chaudhuri, A. *Chem. Soc. Rev.* **2009**, *38*, 3326–3338.
(22) Chen, W. S.; Yan, W. L.; Huang, L. *Cancer Immunol. Immunother.* **2008**, *57*, 517–530.